JOURNAL OF MAGNETIC RESONANCE **133,** 129–133 (1998)
ARTICLE NO. MN981448

Mapping Molecular Orientation in Solids by Rotating-Frame NQR Techniques

F. Casanova, H. Robert, and D. Pusiol

Facultad de Matemática, Astronomía y Física, Universidad Nacional de Córdoba, Ciudad Universitaria, 5000 Córdoba, Argentina

Received July 18, 1997; revised March 18, 1998

A multi-dimensional NQR technique to image both the spatial distribution of quadrupolar nuclei and the local orientation of the electric field gradient tensor at the quadrupole sites in solids is reported. The encoding procedure is based on the irradiation of the sample by a pulse sequence composed of spatially homogeneous and inhomogeneous radiofrequency fields. A method that encodes the spatial and orientation information in the amplitudes of the free-induction decay signals and a proper three-dimensional reconstruction procedure that yields the space-orientation-dependent NQR spectra are described. A two-dimensional variant allows rapid measurement of the spatially dependent orientation distribution of molecules, disregarding the spectroscopic information.

Key Words: **nuclear quadrupole resonance; rotating-frame NQR techniques; NQR imaging.**

INTRODUCTION

To determine physical properties related to inhomogeneities in solids it is important to know the spatial density distribution of the material, the local degree of crystallinity, and the distribution of crystallite orientations for polycrystalline samples.

Images of the spatial distribution of quadrupole nuclei in solids can be produced with the rotating-frame NQR imaging (ρNQRI) technique (*1, 2*). The spatially resolved NQR spectroscopy method (*3, 4*) allows one to correlate information from the spectroscopic and spatial dimensions, thus providing the distribution of local spectral properties of the quadrupole nuclei. In these techniques, spatial resolution is obtained by exciting the sample with a single inhomogeneous radiofrequency (RF) pulse, so that the effective nutation frequency depends on the position with respect to the H_1-field's gradient.

The existence of a molecular orientation distribution in the sample cannot be detected without studying the Zeeman-perturbated quadrupole spectrum in single crystals (*5*). The Zeeman measurements then determine the relative orientations of the molecules with respect to the axes defined by the external perturbative magnetic field.

Harbison *et al.* (*6, 7*) first applied the two-dimensional (2D) nutation NQR Fourier spectroscopy method and demonstrated that it can be used to obtain an orientation-dependent single-crystal spectrum. The nutation method is based on the principle that the radiofrequency transmitter coil introduces an external preferential axis, then the effective RF amplitude experienced by a quadrupolar nucleus depends on the relative orientation of the RF field direction with respect to the principal axes of the quadrupole tensor. The two-dimensional nutation NQR technique uses two time periods: the first interval t_1 is the duration of a homogeneous RF excitation pulse and the second period t is the time of free evolution of a quadrupolar nucleus at zero field. After Fourier transformation against both time variables, t and t_1, separated quadrupolar and nutation spectra along the two frequency axes, ω and ω_1, are obtained. The slices through the 2D spectrum parallel to the ω_1 axis give the function $P(\theta)$ that characterizes the orientation distribution of the electric field gradient (EFG) tensor's axes for the individual sites. The direction of the principal axes of the EFG tensor with respect to axes in the individual molecules can then be obtained approximately from considerations on the molecular structure. When the molecular orientation is not uniform across the sample, the nutation spectrum reflects the average $P(\theta)$ of the material. Then, information about *local* molecular orientation distribution may only be recovered from spatially resolved methods.

In this paper, we report a multi-dimensional NQR technique to spatially resolve orientation and spectroscopic information. The technique is based on the irradiation of the object by a sequence of two RF pulses: a spatially variable RF pulse, of length t_1, encodes the spatial information and a second homogeneous RF field, of duration t_2, enables determination of the orientation distribution. The NQR signal is acquired during a third interval t of free evolution after the pulses. The irradiation sequence is repeated for a full set of equally spaced t_1 and t_2 values, providing a 3D signal $S(t, t_1, t_2)$ that contains the full spectroscopic information correlated with spatial and orientation distribution. A variant of the encoding procedure is presented, which enables one to decrease data acquisition time disregarding the spectroscopic information.

METHODS

The evolution of the quadrupole system is conveniently described in the quadrupole interaction representation (*8*). In

1090-7807/98 $25.00

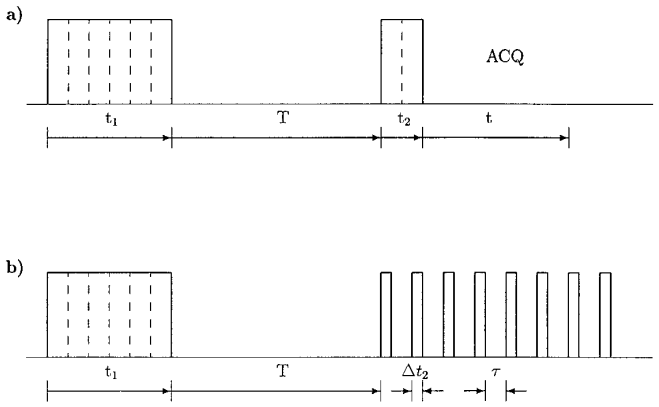

FIG. 1. (a) Pulse scheme for spatially resolving orientation and spectroscopic information. The first pulse of length t_1 is applied with a gradient of H_1 for spatial encoding. The second pulse with duration t_2 applies a homogeneous RF field to encode the orientation distribution of the EFGs. The signal is acquired during the time t. (b) Pulse sequence for rapid two-dimensional nutation spectroscopy that disregards the spectroscopic information. In this variant the step-by-step incrementation of the second pulse is replaced by the train of pulses for rapid rotating-frame sampling.

this picture, the total transformed Hamiltonian for noninteracting spin $I = 3/2$ is given by

$$\mathcal{H}_T = \frac{\Delta\omega}{2}\,\mathcal{L} + \frac{\omega_1'}{2}\,(\mathcal{A}'\cos\alpha + \mathcal{B}'\sin\alpha),$$

where $\Delta\omega = \omega_0 - \omega$ defines the offset between the quadrupole resonance frequency ω_0 and the irradiation frequency ω. The effective nutation frequency is $\omega_1' = \lambda(\theta, \phi)\gamma H_1$, where $\lambda(\theta, \phi) = (2\sqrt{3 + \eta^2})^{-1}\sqrt{(2\eta\cos\theta)^2 + \sin^2\theta(9 + \eta^2 + 6\eta\cos^2\phi)}$. The polar and azimuthal angles, θ and ϕ, define the relative orientation of the axis of the EFG tensor and H_1-field direction, and η is the asymmetry parameter. The operator $\mathcal{L}$ is proportional to the quadrupole Hamiltonian and describes free evolution periods of the quadrupole system. $\mathcal{A}'$ and $\mathcal{B}'$ describe the effects of the RF field with phase $\alpha = 0°$ and $\alpha = 90°$, respectively. Explicit expressions of these operators are given elsewhere (*8*, *9*).

Figure 1a shows the pulse sequence for positional and orientationally resolved NQR spectroscopy. Parallel RF fields, H_1 and H_2, are applied for periods t_1 and t_2 and the free induction decay (FID) signal is acquired in the time t of free evolution. The pulsed H_1 field is applied with a gradient and serves for encoding the spatial information, while the homogeneous RF field H_2 allows us to determine the orientation distribution. The interval T between pulses is much longer than the mean lifetime of coherent spin states (i.e., the transverse relaxation time), but shorter than the spin–lattice relaxation constant, so that the transverse coherences created by the first pulse are destroyed and have no influence on the acquired signal.

The quadrupole system response to the described pulse sequence was easily worked out making use of the relationships reported earlier (*8*, *9*) for the transformation of various operators under the influence of RF and free-evolution Hamiltonians. Because this formalism was extensively used to describe the spin response to several pulse sequences (*2*, *10–12*) no details of the calculations are given.

The local induced signal, calculated as the expectation value of the operator $\lambda(\theta, \phi)(\mathcal{A}'\cos\omega t + \mathcal{B}'\sin\omega t)$, results in

$$G(t, t_1, t_2) = \lambda(\theta, \phi)\cos[\omega_1'(\mathbf{r})t_1]\sin(\omega_2' t_2)\sin[(\omega + \Delta\omega)t].$$

For the sake of simplicity, we restrict the following discussion to the case of an axially symmetric EFG tensor, in which the function $\lambda(\theta, \phi)$ reduces to $\lambda(\theta) = \sqrt{3}/2 \sin\theta$. To consider the effects of a finite width of the NQR resonance line, an integral over a certain distribution $g(\Delta\omega)$ in $\Delta\omega$ should be included. The total induced signal in the receiver coil is the sum of the contributions from all volume elements and local orientations of the EFG tensor's axis, and is given by

$$S(t, t_1, t_2) \sim W(t)\,F(t_1, t_2),$$

where

$$W(t) = \int_{-\infty}^{+\infty} d(\Delta\omega)\,g(\Delta\omega)\sin[(\omega + \Delta\omega)t]$$

describes the conventional FID, and

$$F(t_1, t_2) \sim \int_V d\mathbf{r} \int_0^{\pi/2} d\theta\,\sin^2\theta\rho(\mathbf{r}, \theta) \times \cos[\omega_1'(\mathbf{r})t_1]\sin(\omega_2' t_2). \qquad [1]$$

$\rho(\mathbf{r}, \theta)$ denotes the spatial density of quadrupolar nuclei centered at the coordinate $\mathbf{r}$ with the EFG tensor oriented an angle θ with respect to the RF fields.

In the general case, all of the parameters related to the inhomogeneous H_1 field depend on the spin coordinates $\mathbf{r}$, and the nutation frequency ω_1' should be written as

$$\omega_1'(\mathbf{r}) = \frac{\sqrt{3}}{2}\,\gamma H_1(\mathbf{r})\sin[\theta(\mathbf{r})], \qquad [2]$$

which takes into account the spatial variation in both the magnitude and the orientation of the RF field. The spatially-dependent orientation of the H_1 field can be expressed as $\theta(\mathbf{r}) = \theta + \Delta\theta(\mathbf{r})$, where θ is the orientation of the principal axis system of the EFG tensor with respect to the symmetry axis of the coil (z-axis). Therefore, $\Delta\theta(\mathbf{r})$ measures the departure of the H_1-field's direction relative to the direction defined by the

coil's axis (or z-component of the RF field) and is determined by the component of H_1 perpendicular to the z-axis.

To take into account the nonuniform spatial dependency of the point response function for NQR in Eq. [1], the true distribution of the RF fields needs to be considered. The difficulties related to the coils which arise for NQR imaging of powders are discussed in a paper by Suits and Plude (*13*), and it was suggested that the curvature of the surfaces of constant response might be considered in the image reconstruction technique.

In this work, we assume that the encoding H_1-field varies linearly on the coordinate z and points uniformly in this direction. (This means we are assuming $\Delta\theta/\theta \ll 1$ in Eq. [2].) This is a reasonable assumption if the sample is positioned in a region close to the axis of the coil, so that the curvature of the surfaces of constant field can simply be neglected (*14*). Therefore, the spatial dependency of the nutation frequency simplifies to $\omega_1'(z) = g_1 z \sin\theta$, where the constant g_1 is determined by the strength of the H_1's gradient and the reference point of the spatial coordinate z is chosen at the center of the reversed Helmholtz coil (see under Experiments and Results).

The second nutation frequency is written as $\omega_2' = \omega_{2,0}\sin\theta$, where the constant $\omega_{2,0}$ is given by $\sqrt{3}\gamma H_2/2$ and corresponds to the nutation frequency defined by H_2 for $\theta = \pi/2$.

To reconstruct the 2D function $\rho(z, \theta)$, a set of FIDs for $M_1 \times M_2$ values of t_1 and t_2 is collected. The acquisition time for the complete experiment is then $M_1 \times M_2 \times T_R$, where T_R is the waiting time between each irradiation sequence.

Whenever the spectroscopic information is not relevant, for instance, in quadrupole systems with a single narrow resonance line, a fast encoding procedure can be applied. Figure 1b shows this variant of the encoding scheme, in which the second pulse is replaced by the rapid rotating-frame pulse sequence (SEXI) (*2*). Then, the complete 2D function $F(t_1, t_2)$, is generated by M_1 increments of the value of t_1, and the total acquisition time is reduced to approximately M_1 times the delay between experiments.

The data matrix $F(t_1, t_2)$, from which the function $\rho(z, \theta)$ is obtained, is converted to a two-dimensional spectrum using a cosine Fourier transform with respect to t_1 and a sine Fourier transform along t_2. Then, the 2D-Fourier spectrum exhibits at $\omega_1 = g_1 z \sin\theta$ and $\omega_2 = \omega_{2,0}\sin\theta$ a signal whose amplitude $F(\omega_1, \omega_2)$ corresponds to the spin density $\rho(z, \theta)$ at position z and orientation θ.

The analysis of the 2D spectrum requires a conversion from the frequency domain ω_1 to space domain z. Such a conversion is necessary to eliminate the orientation dependency θ from the spatial dimension and to determine the actual position of the quadrupole nucleus along the RF field gradient. Therefore, the 2D data matrix $F(\omega_1, \omega_2)$ is transformed into a matrix $F(z = K\omega_1, \omega_2)$, where the conversion factor is $K = \omega_{2,0}/(\omega_2 g_1)$. This transformation is easily carried out by computational means.

EXPERIMENTS AND RESULTS

The experiments were performed on a pulsed broadband fully computer-controlled NQR spectrometer (*2*). To produce both homogeneous and inhomogeneous RF fields a coaxial double-coil arrangement was implemented. The probe includes an anti-Helmholtz coil of 18 mm diameter delivering the encoding gradient and a long solenoidal coil of 15 mm diameter that generates the homogeneous RF field and is also used for signal detection. Both resonant circuits are tuned for ^{35}Cl operation at 34.270 MHz. Geometric decoupling of the coils was optimized by minimizing the residual leakage at one coil when the other is fed with a signal at the operation frequency. A fast power switch driven by the pulse programmer was developed to alternate the Kalmus LP1000 power amplifier between the transmitter coils.

For the reconstruction of the 2D spectrum we have implemented a two-dimensional version of the maximum-entropy method (2D-MEM). The implementation of the method for NQR is described in Refs. (*14, 15*). Data processing and spectrometer control is carried out by homemade software running on a Pentium-based personal computer.

Single crystals of paradichlorobenzene, obtained by Bridgeman's method, were used for the present experiments. In the phase α of this compound there are two orientations for the principal axes of the EFG tensor at the ^{35}Cl nucleus site in the unit cell. Therefore, one expects up to two different peaks in the nutation spectrum.

Two disks of 12 mm diameter and 2 mm thickness were cut from different cylindrical single crystals. The orientation distribution for each single crystal was first obtained in separated nutation experiments using the rapid rotating-frame method (*16*). A sequence composed of 64 pulses of 8 μs and a detection interval of 35 μs was applied using the solenoidal coil. Figure 2 shows the Fourier-reconstructed nutation spectra for both samples. From the position of the peaks it is easily determined that the single crystals have different orientation distributions with respect to the external reference system defined by the RF field. The two nutation lines in Figs. 2a and 2b correspond to the two physically inequivalent sites per unit cell. According to the theoretical predictions both the intensities and the positions of the peaks depend on the orientation θ.

To demonstrate the feasibility of spatially resolving an orientation distribution, the second version of the described encoding technique was applied. The NQR object had two cylindrical layers of paradichlorobenzene separated by a 2-mm-thick teflon spacer which provide a simple one-dimensional structure. A set of 32 nutation signals was recorded with the t_1 pulse widths starting at 10 μs and consecutive increments of 10 μs. The train for the rapid acquisition technique was composed of pulses of $\Delta t_2 = 10$ μs and a detection interval of 35 μs. The interval T between the pulses was 3 ms. The total acquisition time for the complete 2D experiment was about 10 min, with 10 transients per irradiation sequence.

From the data matrix $F(t_1, t_2)$ the spectrum of Fig. 3a was reconstructed by the 2D maximum-entropy method. As predicted theoretically the ω_2-dimension contains the orientation distribution in the sample, while the ω_1-axis reflects not only the spatial distribution but also the θ distribution. Figure 3b shows the corrected spectrum following the procedure described under Methods. To do this correction, each value of ω_1, for a given position of ω_2, is multiplied by the factor $\omega_{2,0}/\omega_2$. The parameter $\omega_{2,0}$ was experimentally determined by a nutation experiment carried out on a powder material (the high-frequency edge of the powder nutation lineshape determines the value of $\omega_{2,0}$).

CONCLUSION

Using a two-dimensional nutation spectroscopy method, which combines rotating-frame imaging with nutation NQR spectroscopy, the quadrupolar nuclei density and its EFG's local orientation were simultaneously mapped. A three-dimensional encoding technique was described that allows one to record the full NQR spectroscopic information correlated with spatial and orientation distribution. The technique enables one to image the local degree of crystallinity in solids samples. It should be possible, for instance, to map the changes in the orientation of molecules that take place when phase transition occurs, and it should be feasible to image the domains of the phases.

It is worth pointing out that the proposed technique is suitable for image rendering of single crystals by the rotating-frame NQR method. Because the nutation frequency depends on both amplitude and orientation of the encoding RF field, it is necessary to determine the actual orientation

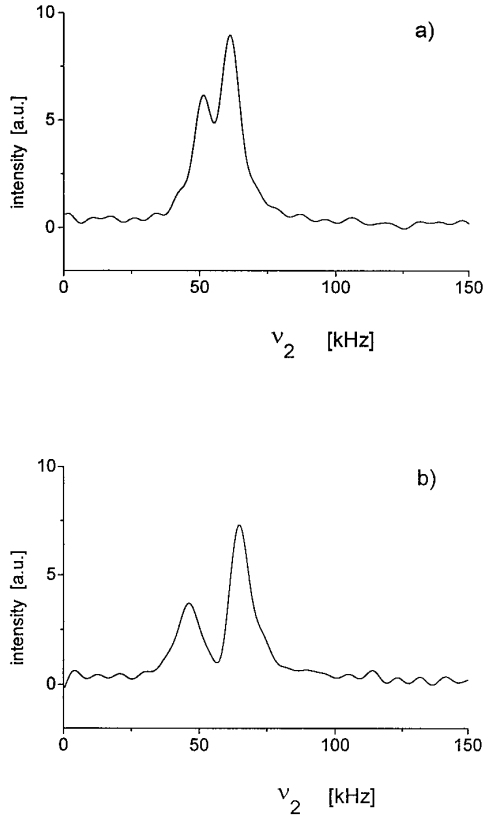

FIG. 2. One-dimensional Fourier-reconstructed nutation spectra of two different single crystals of paradichlorobenzene obtained by the fast 1D nutation encoding technique. The position of the peaks in the spectra (a) and (b) show that different orientation distributions are present.

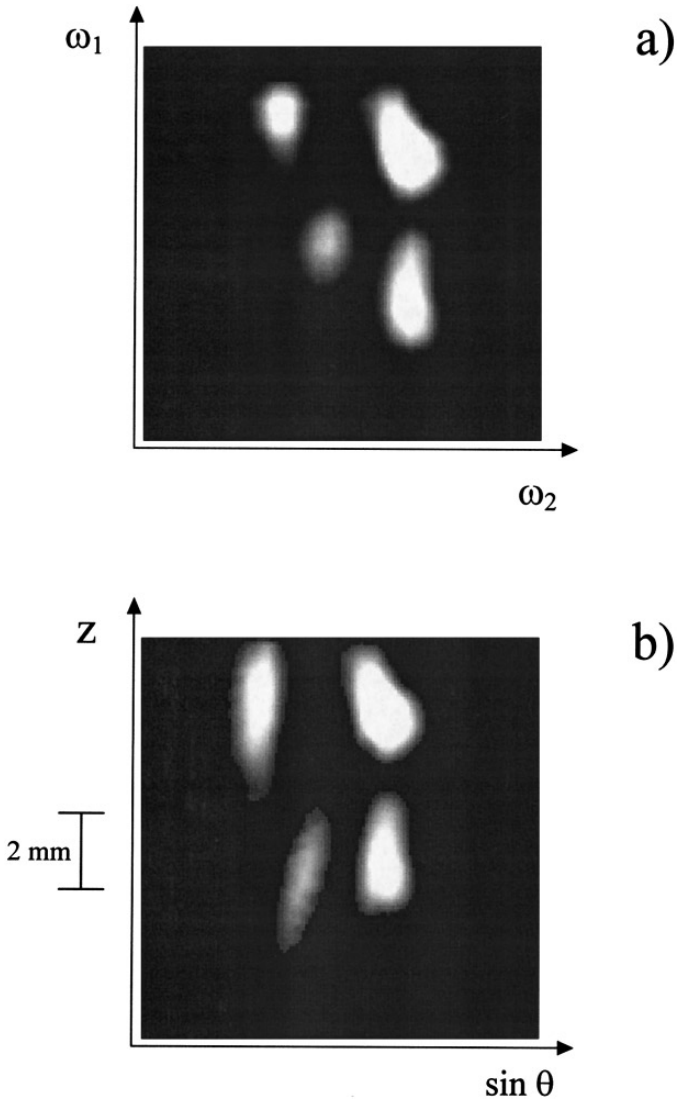

FIG. 3. (a) Two-dimensional spectrum reconstructed by the 2D maximum-entropy procedure for an object composed of two cylindrical single crystals (2 mm thick). To provide a simple 1D structure a 2-mm-thick Teflon spacer was inserted between the pieces of single crystals. The 2D data matrix was recorded using the pulse sequence depicted in Fig. 1b. (b) Spatially and orientationally resolved distribution of quadrupole nuclei for the two-disk object. The spatial dimension was corrected to eliminate the orientation dependence of the effective nutation frequency, following the procedure described in the text.

distribution of the EFG's axis for image reconstruction. Otherwise, the nutation frequency domain will not reproduce the spin density distribution alone. (In fact, the result is like the projection of the spectrum of Fig. 3a along the ω_1-axis.) This problem does not arise with powders because the orientation distribution is assumed to be isotropic in each volume element of the object and can be removed by suitable numerical procedures (*15, 17*).

ACKNOWLEDGMENTS

The authors thank the National and Provincial Research Councils (CONICET and CONICOR), as well as the Fundación Antorchas of Argentina for the financial support of the Project. F.C. and H.R. thank CONICET for Research Fellowships.

REFERENCES

1. E. Rommel, P. Nickel, R. Kimmich, and D. Pusiol, *J. Magn. Reson.* **91,** 630 (1990).
2. H. Robert, A. Minuzzi, and D. Pusiol, *J. Magn. Reson. A* **118,** 189 (1996).
3. E. Rommel, D. Pusiol, P. Nickel, and R. Kimmich, *Meas. Sci. Technol.* **2,** 866 (1991).
4. P. Nickel, H. Robert, R. Kimmich, and D. Pusiol, *J. Magn. Reson. A* **111,** 191 (1994).
5. T. P. Das and E. L. Hahn, *Solid State Phys.* Suppl. 1 (1958).
6. G. S. Harbison, A. Slokenbergs, and T. M. Barbara, *J. Chem. Phys.* **90,** 5292 (1989).
7. G. S. Harbison and A. Slokenbergs, *Z. Naturforsch* **45A,** 575 (1990).
8. J. C. Pratt, *Mol. Phys.* **34,** 539 (1977).
9. A. J. Vega, *Isr. J. Chem.* **32,** 195 (1992).
10. Sunyu Su and R. L. Armstrong, *J. Magn. Reson. A* **101,** 265 (1993).
11. A. Ramamoorthy, N. Chandrakumar, A. K. Dubey, and P. T. Narasimhan, *J. Magn. Reson. A* **102,** 274 (1993).
12. A. K. Dubey, A. Ramamoorthy, and P. Raghunathan, *Chem. Phys. Lett.* **168,** 401 (1990).
13. B. H. Suits and G. Y. Plude, *J. Magn. Reson. A* **117,** 84 (1995).
14. H. Robert and D. Pusiol, *J. Magn. Reson.* **127,** 109 (1997).
15. H. Robert, D. Pusiol, E. Rommel, and R. Kimmich, *Z. Naturforsch* **49A,** 35 (1994).
16. H. Robert and D. Pusiol, *J. Chem. Phys.* **106,** 8 (1997).
17. E. Rommel, R. Kimmich, H. Robert, and D. Pusiol, *Meas. Sci. Technol.* **3,** 446 (1992).